

QCD at finite density

Sourendu Gupta*

*Dept. of Theoretical Physics, Tata Institute of Fundamental Research, Homi Bhabha Road,
Mumbai 400005, India.*

E-mail: sgupta@tifr.res.in

Developments in QCD at finite density are reviewed. I begin by discussing some new algorithms which have been applied to other theories with sign problems. Then I discuss the method of analytic continuation in QCD using a series expansion and review some of the results obtained using this method. By now there are several different simulations using the method, and together they give estimates of the systematic lattice effects, which turn out to be controlled. Finally I discuss a direct comparison of some of these lattice predictions with new experimental data which results in a very pleasant agreement.

*The XXVIII International Symposium on Lattice Field Theory, Lattice2010
June 14-19, 2010
Villasimius, Italy*

*Speaker.

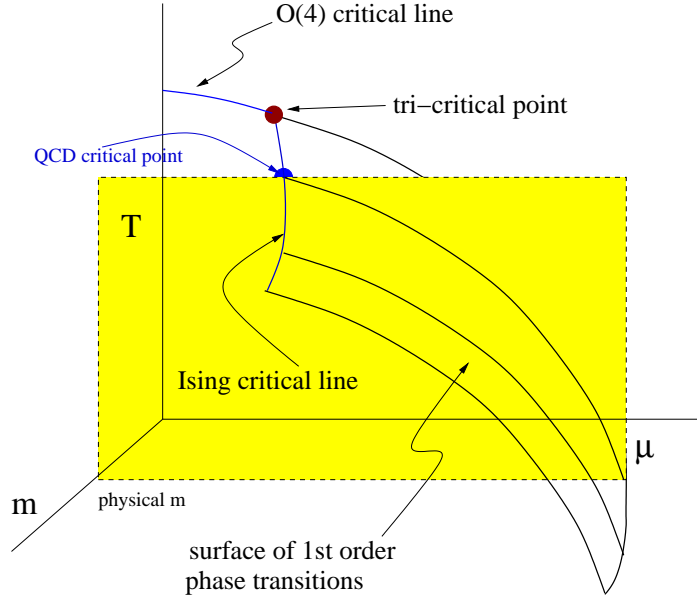


Figure 1: A conjectured phase diagram of QCD for $N_f = 2$ and for $N_f = 2 + 1$ when the strange quark mass is not much smaller than Λ_{QCD} . In the chiral limit there is a tri-critical point, from which emerges an Ising critical line whose intersection with the plane of physical quark mass is the QCD critical point.

1. Introduction

QCD at finite baryon density is interesting because of two reasons: first that there is a program of experimental studies covering five colliders, running and planned, which will look at this problem, and second, that it does not seem open to standard methods of attack in lattice gauge theory due to a sign problem [1]. In this review I will bring together evidence that the problem is still open to a fruitful attack using small modifications of the usual tools of lattice gauge theory, and give some of the main physics results. The context of these first results is the conjectured phase diagram of Figure 1 [2].

Any Monte Carlo integration process suffers from a sign problem if the integrand is not real and positive definite. For the QCD action with a chemical potential on the baryon number, the determinant of the Dirac operator, which is the quark part of the measure, obeys the condition

$$\det(D + m + \mu \gamma_0)^* = \det(D + m - \mu^* \gamma_0), \quad (1.1)$$

where D is the massless Dirac operator, m is the mass, μ is the baryon chemical potential, and $*$ denotes complex conjugation. For any generic complex chemical potential this shows that there is a sign problem. For pure imaginary μ (including $\mu = 0$), the determinant is real, and one can further prove its positivity by considering its commutation with γ_5 .

This sign problem is not necessarily mild. Baryonless random matrix theory seems to predict that for $\mu < m_\pi/2$ the distribution of signs is Gaussian and becomes Lorentzian at larger μ [3]. In either case the problem is severe. An earlier work had estimated the contours of the variance of the phase of the quark determinant and found that this decreases at high temperatures, where the problem could therefore become easier [4].

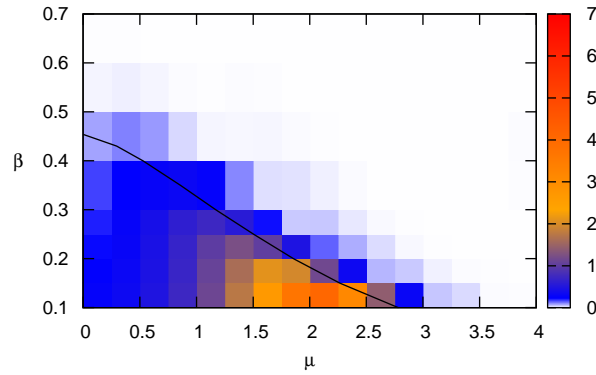


Figure 2: The line is the phase boundary of the 3d XY model, found using the worm algorithm [8]. The instability of the complex Langevin method is illustrated in this figure [11]: this method converges to the wrong probability measure. The difference between the actions for the true and converged distributions is colour coded.

This review is structured as follows. Section 2 presents an overview of very interesting new attempts to attack the sign problem directly; unfortunately they are not yet at the stage where they can be applied to QCD. Section 3 reviews the Madhava-Maclaurin series expansion¹ method which has yielded first results on the phase diagram and on some other measurable quantities. Finally in Section 4 first results from experiments are reported along with comparisons to lattice QCD predictions.

2. Trial algorithms

The class of algorithms which has had the most attention till now is reweighting: perform the Monte Carlo procedure at a point in the phase diagram where there is no sign problem, and then find expectation values of operators by choosing an appropriate weight for each configuration. Various problems with this process are by now well-known; they include large errors due to cancellations and inaccurate sampling, which become exponentially large with the volume. The Budapest group applied this method to the problem of locating the QCD critical point [5]. The Bielefeld-Swansea algorithm is a variant of this method which expands the determinant in a series in μ [6]. There have been no developments in this class of algorithms since it was reviewed in 2008 [7].

Two new classes of algorithms are being tested currently, and, although their applicability to QCD is not yet clear, they are interesting enough to merit some discussion. Interestingly, they become easy to compare because the two algorithms have been, deliberately, applied to the same model recently. This is the 3-d XY model at finite chemical potential, which has the action

$$S = -\beta \sum_{x, \hat{\mu}} \cos(\theta_x - \theta_{x+\hat{\mu}} - i\mu \delta_{\hat{\mu}, \hat{t}}). \quad (2.1)$$

¹ In the 14th century Madhava of Sangamagrama developed the series expansion for functions and estimates of the error terms which later came to be associated with the name of Maclaurin.

This suffers from a sign problem when $\mu \neq 0$.

One approach [8] exploits the fact that sign problems are not inherent to the physics of a system, but to specific representations. By a clever transformation of fields which amounts to redefining the theory in terms of fluxes of particles along links, they reduce it to a form without a sign problem, although the theory then becomes non-local. However, in this representation it becomes amenable to a numerical attack using the “worm algorithm” [9]. This work then sets out a finite-size scaling theory which describes the point at which it becomes energetically favourable to add one more particle to the ground state. The simulation results allow the extraction of finite size scaling parameters which can then be used to determine the phase diagram.

The other approach resurrects an old idea— the complex Langevin method, wherein one addresses sign problems by complexifying the fields while the noise remains real. Earlier works had been plagued by runaway directions and associated numerical instabilities, now brought under control by the use of adaptive step-size integrators. For a while a proof of convergence of such methods seemed to be within reach [10]. However, it turns out that there may be a convergence to the wrong result [11]. This is illustrated in Figure 2, which shows that the problem arises mainly at small temperature and large chemical potential. Since this region is similar to that in which QCD has large sign fluctuations [3], a better understanding of the origin of this problem may throw light on applications to QCD.

In the next section we turn to the algorithm, first described in [13], which is now used by many groups, and has begun to yield many consistency tests and, possibly, even contact with experiment.

3. The Madhava-Maclaurin series expansion

The pressure of QCD matter in a grand canonical ensemble can be expanded in a Madhava-Maclaurin series around the point $\mu = 0$ to obtain

$$P(T, \mu) = P(T) + \frac{\mu^2}{2!} \chi^{(2)}(T) + \frac{\mu^4}{4!} \chi^{(4)}(T) + \dots \quad (3.1)$$

where all the coefficients are computed at $\mu = 0$. $P(T)$ is the pressure at zero chemical potential, $\chi^{(2)}(T)$ is called the quark number susceptibility (QNS) [12] and all the $\chi^{(n)}(T)$ are generically called non-linear susceptibilities (NLS). It was suggested that the NLS could be measured in $\mu = 0$ simulations, and the feasibility was demonstrated by computations in quenched QCD [13]. More recently, within the last year, there have been attempts to compute these coefficients by simulating QCD at imaginary chemical potential and fitting extrapolating functions to the data [14] (we will return to a discussion of this later).

3.1 Computational effort

The $\chi^{(n)}$'s are combinations of quarks loops with insertions of γ_0 up to n times [15]. These quark loop traces are obtained through stochastic noise averages. One measure of the feasibility of such measurements is to examine the signal to noise ratio in the measurements when the number of noise vectors is N_v , *i.e.*, the ratio of the mean and square root of the variance of such a trace in one configuration. When the ratio is large, the measurement is easy. Such a measure was reported using staggered quarks on a 4×24^3 lattice at $T/T_c = 0.75$ and $N_f = 2$ when the quark mass is

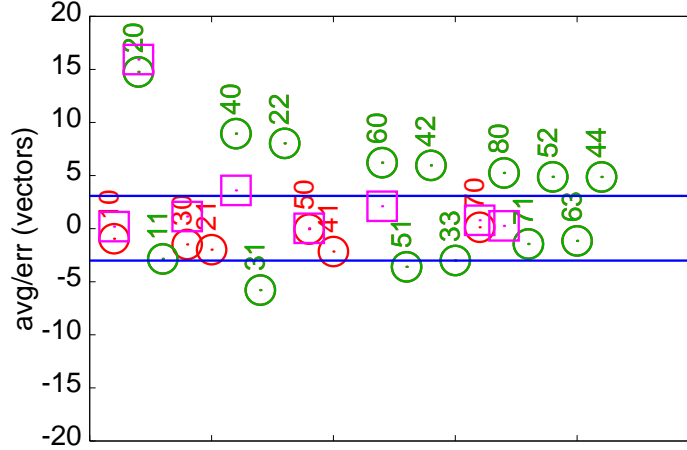


Figure 3: Signal to noise ratios for various fermion traces which enter the evaluation of the NLS (see [15] for explanations of the notation). Circles denote data for staggered quarks [15] and boxes for P4 quarks [16]. The red circles denote measurements of quantities which should be exactly zero.

tuned to give $m_\pi = 230$ MeV [15]. Here we add results from P4 action with $N_f = 2 + 1$, with light quark masses tuned to the same value of m_π and $T/T_c = 0.84$ [16]. In both cases $N_v = 400$ and the signal to noise ratios are comparable (see Figure 3). A direct comparison with Asqtad quarks is not available, but from the claim that 50% of the noise in [17] is due to stochastic estimators, one finds that the signal to noise ratio for that Dirac operator is comparable.

Near T_c autocorrelations between successive configurations is large— of the order of 200–250 trajectories. Assuming that it takes about 200 fermion matrix inversions per trajectory, and that we use $N_v = 500$ for every decorrelated configuration, then, since it takes 18 inversions per measurement (up to the 8th order of the expansion in eq. 3.1), the ratio of CPU times for a measurement to that for generating a decorrelated configuration is 0.24. The marginal cost of measurement is small. Well inside the hot phase, at $2T_c$, the autocorrelation time drops to about 4 trajectories, whereas $N_v = 100$. The ratio of CPU times for measurement to generating decorrelated configurations climbs to 4.5, however, with relatively small expenditure of CPU time. As a result, direct measurements of the NLS are highly feasible. An added attraction is that configurations which have been generated for any finite temperature study can be reused for such analysis, thus reducing the marginal cost even further.

3.2 Series Analysis for the critical point

Methods for analysis of series expansions of the free energy or its derivatives are well-known in statistical mechanics, and have been used successfully in many cases [18]. While the core of the analysis is the same, there are interesting differences between these older works and the application to QCD, which lead to differences in the method of analysis [15, 19]. The series coefficients in the older works came from exact enumeration of graphs, corresponding to infinite volume systems, so that a coefficient was either known exactly or not known. In the present case the series coefficient is evaluated on finite lattices with statistical errors through a Monte Carlo process.

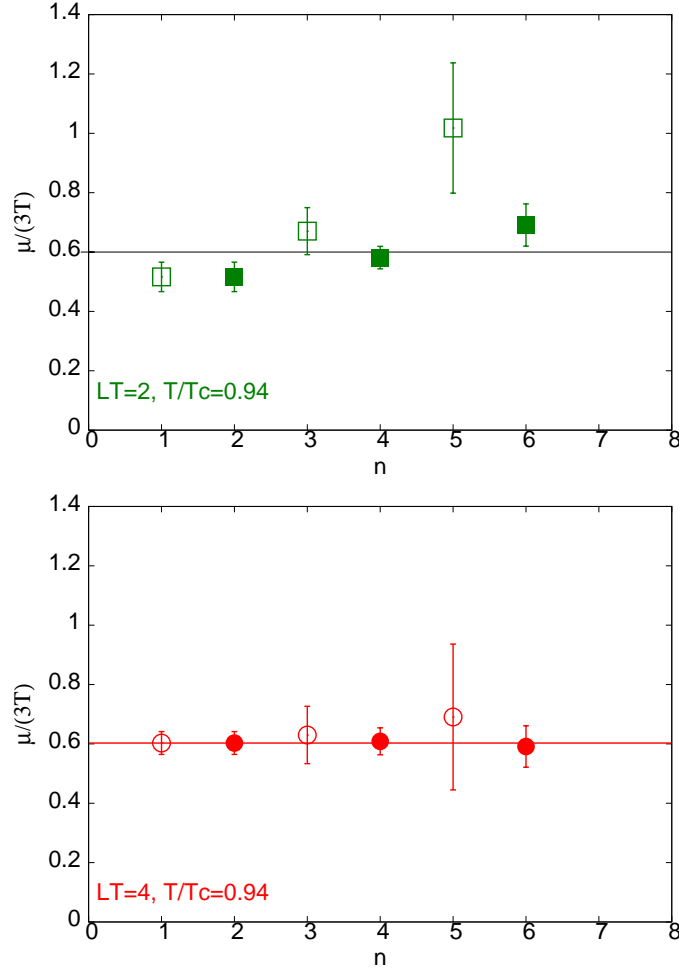


Figure 4: Estimates of the radius of convergence of the series expansion in eq. 3.2 from finite temperature simulations at $T = 0.94T_c$ with two flavours of staggered quarks and the bare quark mass tuned to give $m_\pi = 230$ MeV and lattice spacing $1/(6T)$. Open symbols correspond to estimates of z_n^* and filled symbols to z_n^* . When LT increases from 2 to 4 $n_*(L)$ increases significantly, as shown.

The main point of the analysis is that the series for the quark number susceptibility can be analyzed for its radius of convergence. The series for the QNS is

$$\frac{\chi^{(2)}(T, \mu)}{T^2} = \frac{\chi^{(2)}(T)}{T^2} + \frac{z^2}{2!} \chi^{(4)}(T) + \frac{z^4}{4!} T^2 \chi^{(6)}(T) + \dots \quad (3.2)$$

where $z = \mu/T$ and each of the dimensionless combinations $T^{n-4} \chi^{(n)}(T)$ is the direct output of a lattice computation. Since the expansion is in z at fixed value of T , it is equivalent to an expansion in μ . If the divergence occurs at a temperature at which all the series coefficients are positive, then the non-analyticity occurs for real values of z , and the divergence can be identified with the critical point of QCD.

The radius of convergence can be found by several methods, all of which correspond to com-

paring the series against another with a known singularity. The best known definitions are—

$$z_{n+1}^* = \sqrt{\frac{n!T^{n-2}\chi^{(n+2)}}{(n+2)!T^{n-4}\chi^{(n)}}}, \quad \text{and} \quad \bar{z}_n^* = \left(\frac{2!T^{n-4}\chi^{(n)}}{n!\chi^{(2)}/T^2} \right)^{1/(n-2)}. \quad (3.3)$$

The star and bar do not indicate complex conjugation. The common limit as $n \rightarrow \infty$ of both is the radius of convergence of the series. This test is closely coupled to a finite volume scaling analysis.

The reason is the following. If there is a critical point at some (μ^E, T^E) then the QNS diverges there on an infinite volume system. However, on any finite volume, L^3 , there may be a peak, but no divergence. As the system size decreases, the peak becomes broader and lower. As a result, z_n^* and \bar{z}_n^* may seem to give a finite radius of convergence for $n < n_*(L)$. For larger n both z_n^* and \bar{z}_n^* will then become larger and larger, since there is no actual divergence in the series for the QNS. As L increases, one would find $n_*(L)$ also increasing without limit. In simulations of QCD with 2 flavours of staggered quarks with the bare quark mass tuned to give $m_\pi = 230$ MeV, such behaviour is actually seen at one temperature (see Figure 4). At this temperature all the NLS are positive, so the limiting singularity is at real values of μ . We can then identify such a temperature with T^E and the corresponding estimate of the radius of convergence with μ^E/T^E .

Such estimates of the critical point have been made with two different lattice spacings using two flavours of staggered quarks on large volume lattices [15, 19]. A computation with 2+1 flavours of P4 quarks at almost the same value of m_π has also been performed with large lattices [20] and preliminary estimates of the radius of convergence have been reported [21]. These are collected in Figure 5. Since large volumes are crucial to obtaining a stable estimate of the critical point, older computations with smaller volumes have not been added into this figure even if they have realistic values of m_π . A by-product of this choice is that all the points in the figure use the same computational technique, albeit with different lattice spacings and quark actions.

Interest in the critical point is enhanced because of the possibility that heavy-ion collision experiments may observe it. Fireballs produced in such collisions undergo chemical freezeout at certain values of μ and T which change with the center-of-mass energy, \sqrt{S} , of the colliding nuclei. The chemical freezeout point is relevant if one tries to use fluctuations of conserved quantum numbers as probes of the critical point: we shall return to this argument later. The freezeout curve is parametrized in [24]. This has been superposed on the phase diagram in Figure 5 by using the scale $T_c = 175$.

A pleasant fact emerges from Figure 5: that lattice spacing effects can be bounded in magnitude by currently available computations. The difference between different kinds of actions is, of course, a finite lattice spacing artifact. The magnitude of the lattice spacing effect estimated from two different spacings with the same action turns out to be comparable with that from a comparison of two different actions at nearly the same lattice spacing.

Interestingly, the effect of the strange quark on the end point seems to be under control. It has long been known that in the Columbia plot, the physical point corresponds to a thermal cross over [22], as a result of which the topology of the phase diagram of realistic 2+1 flavour QCD is the same as for two flavours, as in Figure 1. As the strange quark mass is increased and the light quark mass is reduced, the thermal crossover passes through a critical point into a first order transition. It turns out that the line of critical points is far from the physical point: the pion needs to be about

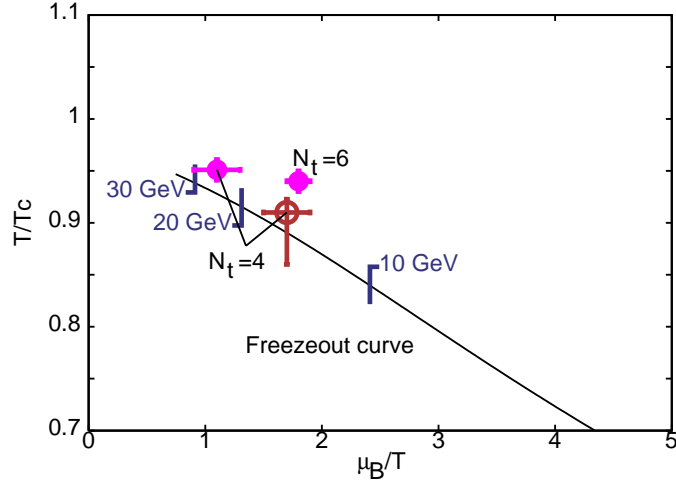


Figure 5: Estimates of the critical point of QCD from lattice computations with $m_\pi \simeq 230$ MeV and $Lm_\pi > 4$. The points in pink are obtained from computations with 2 flavours of staggered quarks and the point in brown from 2+1 flavour P4 quarks. The values of μ and T along the freezeout curve are parametrized by [24] and have been used in conjunction with $T_c = 175$. Some values of \sqrt{S} have been marked along the freezeout curve.

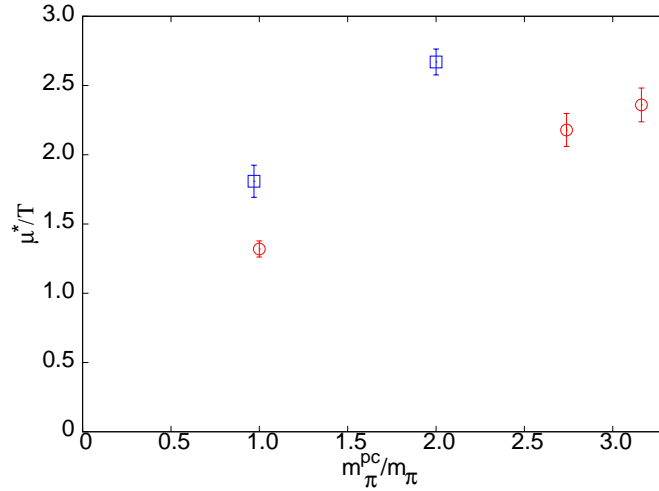


Figure 6: The variation of the radius of convergence with in partially quenched computations with the staggered sea quark mass tuned to give $m_\pi \simeq 230$ MeV. As the valence quark mass is changed the partially quenched pion mass is m_π^{pc} .

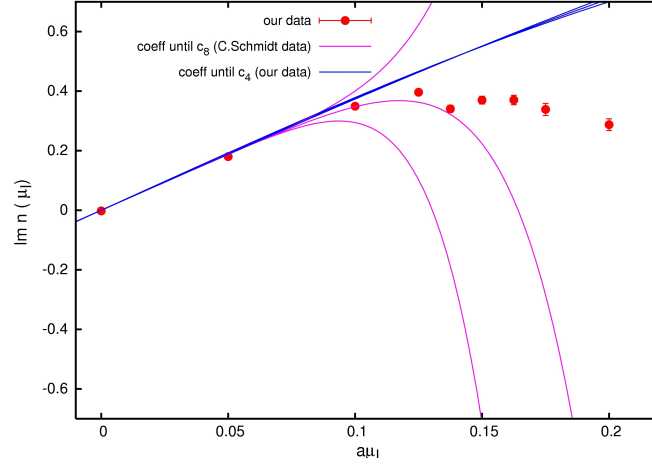


Figure 7: Using the series expansion to describe the data obtained through direct simulations at imaginary chemical potential.

10 times lighter and the strange quark mass about 3 times lighter [23]. This could be one reason to suspect that the numerical values for the critical end point in 2 flavour and 2+1 flavour QCD may not be very different. Such an argument is compatible with the results collected in Figure 5.

The major remaining effect is due to the light quark mass being larger than physical. The only exploration of this effect till now is a partially quenched computations with $a = 1/(4T)$ and two flavours of staggered quarks with a sea quark mass tuned to give $m_\pi = 230$ MeV [25]. Interestingly, an interpolation between the measured value of the radius of convergence was consistent with the result of an unquenched computation with P4 quarks tuned to give $m_\pi = 550$ MeV [4]. In Figure 6 the earlier results are extended by adding a similar analysis for $a = 1/(6T)$. The extrapolation to the physical value of m_π shows a 15% drop in the value of μ^E .

3.3 Extrapolation of observables

Apart from the prediction of the critical point, the series expansion could be used to extrapolate measurements to finite chemical potential. Tests of such extrapolations are whether they can describe measurements made directly through simulations at imaginary chemical potential. The most straightforward extrapolation is to use the series. A preliminary attempt [27] is shown in Figure 7. One sees that adding new terms in the series improves the extrapolation only marginally in μ . Closely related to this exercise are attempts to extract the series coefficients from measurements obtained in direct simulations at imaginary chemical potential. It was shown recently [14] that simple series descriptions of the data obtained at finite imaginary chemical potential are inefficient and more complicated forms are needed to perform the extraction of the series coefficients.

Clearly, when the series expansion of a physical quantity is close to divergence, then a truncated sum is clearly not the best way to find the value of this quantity at finite μ . One must search for series resummation techniques. One method which has been widely used for resummation of high temperature series of spin models [18] is to determine Padé approximants using them. There

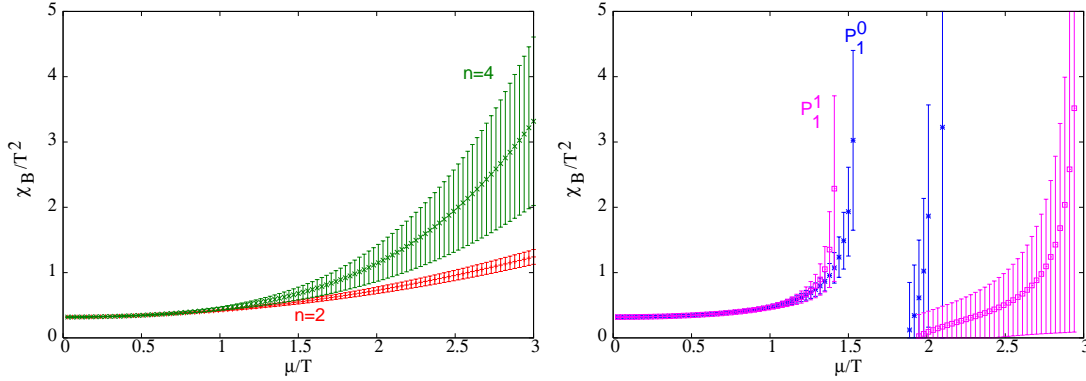


Figure 8: Extrapolation of the measurement of the QNS at T^E to finite μ . The series resummation does not diverge, although adding terms causes large changes. The Padé approximant exhibits the divergence but is stable under addition of extra terms.

is a detailed theory of Padé approximants [26] which needs to be extended to applications in QCD where the series coefficients are known only within some statistical errors [19].

In Figure 8 we show truncated series sums for the QNS at $T^E = 0.94T_c$. There is no sign of any divergence, although successive orders fail to agree with each other as the radius of convergence is approached. In the same figure we also show the QNS obtained with Padé resummations of the series. These exhibit the divergence identified through series analysis. It is also useful to note that the Padé approximants fitted to different number of terms of the series agree with each other except when z is significantly larger than the radius of convergence. The Padé analysis indicates a width of the critical region which is about $\Delta\mu/T^E \simeq 0.25$.

4. Comparison with experiments

The QNS are related to fluctuations of conserved quantities in a grand canonical ensemble. It may be possible to realize this in an experiment by looking at a part of the fireball produced in a heavy-ion collision, provided it thermalizes. Then one way in which grand canonical physics can be extracted is by observing particles only in a restricted space-time rapidity range. If this range is chosen judiciously, then the remainder of the fireball may act as a heat-bath for the system under observation. Then each collision event satisfying the above experimental cuts is one member of a grand canonical ensemble of events.

Event-to-event distributions of conserved quantities then form the observables of interest [28]. The cleanest observable is the distribution of total electric charge, Q , since there is very little chance of missing a significant fraction of the charge within the acceptance volume V . Baryon number, B , and strangeness, S , are also good observables, but since there are uncharged baryons as well as long-lived uncharged strange particles, both of which are missed by detectors, the connection to these quantities is made at a further remove [29]. Nevertheless, currently the most extensive data comes from observations of the net proton number, which is a proxy for the net baryon number.

It is seen that fluctuations of conserved quantities are Gaussian. The first question is whether this Gaussian is entirely (or largely) due to thermal fluctuations. The only way to answer this

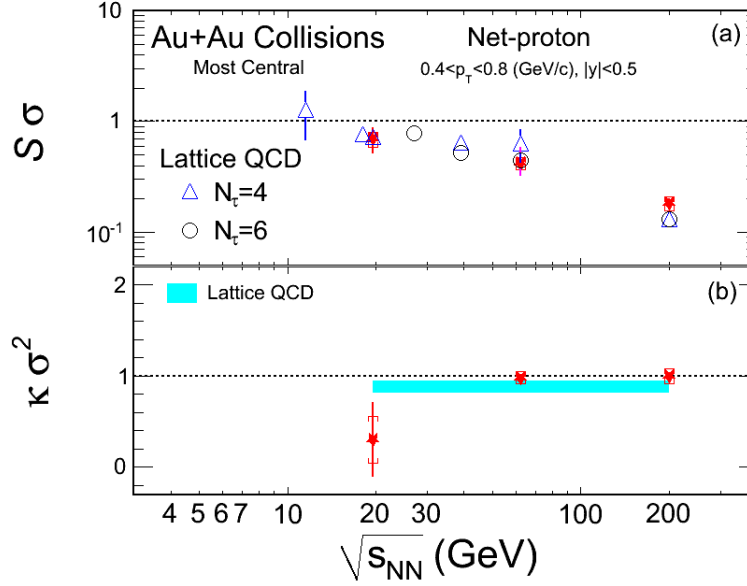


Figure 9: Comparison of experimental data with lattice predictions. The upper panel shows m_1 and the lower m_2 .

is by going beyond the Gaussian. A systematic way to do this is to change V and check how the distribution changes. Gaussian distributions usually arise in experiments through a process described by the central limit theorem: with increasing V the higher cumulants of the distribution scale down with larger powers of V . The STAR collaboration reported such a measurement [30] using an experimentally determined parameter called the participant number, N_{part} , as a proxy for V . At small N_{part} all the cumulants, $[B^n]$, are comparable, and with increasing N_{part} the scaling of the cumulants is exactly as one should expect— in other words, the microscopic physics encoded in the set of $[B^n]$ does not change with N_{part} .

If the fluctuations are due to thermal processes, then $[B^n]$ are related to various NLS computable in QCD. This is the next step: to check the data against the predictions [31]. In order to do this one has to take combinations of the cumulants which are free of incidental variables such as the unmeasurable V . This is achieved by taking the ratios

$$m_1 = \frac{[B^3]}{[B^2]} = \frac{T\chi^{(3)}(T, \mu)}{\chi^{(2)}(T, \mu)}, \quad m_2 = \frac{[B^4]}{[B^2]} = \frac{T^2\chi^{(4)}(T, \mu)}{\chi^{(2)}(T, \mu)}, \quad m_3 = \frac{[B^4]}{[B^3]} = \frac{T\chi^{(4)}(T, \mu)}{\chi^{(3)}(T, \mu)}, \quad (4.1)$$

Now, the left hand side of each equation is known from experiment at each \sqrt{s} , and the right hand side is known from lattice computations if one knows the freezeout values of μ and T . These values are parametrized from experimental data in [24] assuming that the fireball thermalizes.

On one hand, the series expansions for the NLS are known from the expansion in eq. 3.1, on the other, the ratios of eq. 4.1 have well-determined power behaviour at small z , and poles near the critical point. As a result, resummation of the series by Padé approximants is possible. The

parameters in the Padé approximants are closely related to the estimates of z_n^* . As a result, the lattice artifacts in $m_{1,2,3}$ are related to those already discussed in the previous section. It turns out that both m_1 and m_2 may have significant finite lattice spacing corrections: mainly a common finite multiplicative factor which is also the correction to the estimate to the radius of convergence. For m_3 lattice spacing corrections are small, except in the vicinity of the critical point. Results for these quantities have been given in [33].

The STAR experiment at RHIC has recently published a measurement of comparable quantities from runs at three different values of \sqrt{s} where comparisons with these quantities are presented [32]. As shown in Figure 9, it turns out that there is good agreement between the data and the predictions. Many questions remain to be answered: on the side of the lattice computations the usual questions about flavours, quark masses and lattice spacing, on the experimental side about the removal of non-thermal backgrounds and other sources of fluctuations. Nevertheless, this is a significant milestone: the first direct comparison of heavy-ion data with lattice predictions. In future such a comparison may even yield a direct measurement of T_c as pointed out in [33], allowing us to set the scale for lattice measurements in an entirely new way.

5. Assorted topics

There are various developments at finite chemical potential which cannot be covered fully here because of space constraints. However, they are interesting in their own right and have useful connections to the physics which is discussed in the previous sections. Here I make a brief mention of some of these works.

In the chiral limit there is a line of second order phase transitions at finite μ , emanating from the finite temperature critical point (see Figure 1). The curvature of this line is an object of interest because it sets a scale for the tricritical temperature in the chiral limit. Interesting new work was presented on this problem by several groups [34].

The phase diagram at imaginary chemical potential is of some interest, since it has to be understood if simulations in this region are to be used for analytic continuation to the physically interesting case. New results were presented by two groups [35].

The investigation of correlation functions at finite chemical potential is in its infancy [36]. Any new information is interesting at this stage. New work was reported in this meeting [37].

The strong coupling expansion has been resurrected in this context and improved techniques are now being used to investigate the phase diagram. Interesting new results in this direction were reported [38]. These may serve to benchmark future simulations using the worm algorithm which can be adapted to the strong coupling theory.

All the results reported till now simulate the grand canonical ensemble. Very little systematic effort has gone into simulations in the canonical ensemble with fixed baryon number. One such attempt was reported [39].

6. Conclusions

Over the years there has been a great improvement in the understanding of the sign problem at finite μ in QCD: where it could be tractable and where it is not [3]. There has been little progress

in directly tackling this problem, although there are interesting developments in the handling of other models with sign problems [8, 11]. However, in the last five years there has been enormous progress in lattice computations which can yield information on QCD at finite μ . The essential development is the use of analytic continuation, through a Madhava-Maclaurin series expansion in μ [13]. There are encouraging tests of this method in performing analytic continuation to finite imaginary μ where direct simulations are also possible [14, 27].

The series expansion method has been applied to the extraction of the QCD critical point at various lattice spacings [15, 19] and with various quark actions and numbers of flavours [20, 17]. A composite figure of the predictions is given in Figure 5. It is clear from this figure that the method yields results with controlled statistical and systematic errors. Since the results are not strongly sensitive to the choice of action, it is also clear that lattice spacing effects are bounded.

An interesting development in the past year has been the proposal of a set of measurables, eq. 4.1, which allow a direct comparison of experiment and lattice computations. First results show very good agreement between data [32] and prediction [33]. This calls for renewed activity in this field and a greater scrutiny of the known systematic uncertainties which need control.

For communicating their results and then patiently answering my questions I would like to thank Gert Aarts, Shailesh Chandrasekharan, Rossella Falcone, Maria-Paola Lombardo, and Christian Schmidt.

References

- [1] Ph. de Forcrand, *PoS LATTICE2009* (2009) 010 [arxiv:1005.0539].
- [2] M. A. Stephanov, K. Rajagopal and E. V. Shuryak, *Phys. Rev. Lett.* 81 (1998) 4816, and *Phys. Rev. D* 60 (1999) 114028.
- [3] M.-P. Lombardo, K. Splittorff and J. Verbaarschot, *Phys. Rev. D* 80 (2009) 054509 [arxiv:0904.2122].
- [4] C. R. Allton *et al.*, *Phys. Rev. D* 71 (2005) 054508 [hep-lat/0501030].
- [5] Z. Fodor and S. Katz, *Phys. Lett. B* 534 (2002) 87 [hep-lat/0104001].
- [6] C. R. Allton *et al.*, *Phys. Rev. D* 66 (2002) 074507 [hep-lat/0204010].
- [7] S. Ejiri, *PoS LATTICE2008* (2008) 002.
- [8] D. Banerjee and S. Chandrasekharan, [arxiv:1001.3648].
- [9] For more on this class of algorithms see the reviews S. Chandrasekharan, *PoS LATTICE2008* (2008) 003 [arxiv:0810.2419]; U. Wolff, *Lattice2010*
- [10] G. Aarts, E. Seiler, I. O. Stamatescu, *Phys. Rev. D* 81 (2010) 054508 [arxiv:0912.3360].
- [11] G. Aarts and F. A. James, *J. H. E. P.* 1008 (2010) 020 [arxiv:1005.3468].
- [12] S. A. Gottlieb *et al.*, *Phys. Rev. Lett.* 59 (1987) 2247.
- [13] R. V. Gavai and S. Gupta, *Phys. Rev. D* 68 (2003) 034506 [hep-lat/0303013].
- [14] P. Cea *et al.*, *Phys. Rev. D* 80 (2009) 034501 [arxiv:0905.1292];
- [15] R. V. Gavai and S. Gupta, *Phys. Rev. D* 71 (2005) 114014.
- [16] C. Schmidt, private communication.

- [17] C. DeTar *et al.*, *Phys. Rev. D* 81 (2010) 114504 [arxiv:1003.5682].
- [18] C. Domb and M. S. Green, *Phase Transitions and Critical Phenomena*, vol 2, Academic Press, (1972).
- [19] R. V. Gavai and S. Gupta, *Phys. Rev. D* 78 (2008) 114503.
- [20] M. Cheng *et al.*, *Phys. Rev. D* 79 (2009) 074505.
- [21] C. Schmidt, arXiv:1007.5164.
- [22] F. R. Brown *et al.*, *Phys. Rev. Lett.* 65 (1990) 2491.
- [23] G. Endrodi *et al.*, *PoS LAT2007* (2007) 182 [arxiv:0710:0998].
- [24] H. Oeschler *et al.*, *PoS CPOD2009* (2009) 032.
- [25] R. V. Gavai and S. Gupta, *Nucl. Phys. A* 785 (2007) 18.
- [26] G. A. Baker and P. Graves-Morris, *Encyclopedia of Mathematics: Padé Approximants*, Vol 13, Part 1, Addison-Wesley Publishing Company, Reading, Massachusetts, (1981).
- [27] R. Falcone *et al.*, these proceedings.
- [28] M. Asakawa, U. W. Heinz and B. Muller, *Phys. Rev. Lett.* 85 (2000) 2072; S. Jeon and V. Koch, *Phys. Rev. Lett.* 85 (2000) 2076.
- [29] Y. Hatta and M. A. Stephanov, *Phys. Rev. Lett.* 91 (2003) 102003.
- [30] B. Mohanty, *Nucl. Phys. A* 830 (2009) 899c.
- [31] S. Gupta, *PoS CPOD2009* (2009) 025.
- [32] M. M. Aggarwal *et al.*, (STAR Collaboration) *Phys. Rev. Lett.* 105 (2010) 022302.
- [33] R. V. Gavai and S. Gupta, arXiv:1001.3796.
- [34] S. Ejiri *et al.*, arXiv:1011.4747 (these proceedings); S. Mukherjee *et al.*, arXiv:1012.2231 (these proceedings); B. Klein *et al.*, arXiv: 1011.1435 (these proceedings).
- [35] O. Phillipsen *et al.*, these proceedings; L. Cosmai *et al.*, these proceedings.
- [36] S. Choe *et al.*, *Phys. Rev. D* 65 (2002) 054501; S. Gupta, eprint hep-lat/0202005.
- [37] H. Iida *et al.*, arXiv: 1012.2044 (these proceedings).
- [38] K. Miura *et al.*, arXiv:1010.5687 (these proceedings).
- [39] K.-F. Liu *et al.*, these proceedings.